Predictions for dijet production in DIS
using small x dynamics

J. Kwiecinski[a,b], A.D. Martin[b] and A.M. Stasto[a,b]

[a] H. Niewodniczanski Institute of Nuclear Physics, ul. Radzikowskiego 152, Krakow, Poland
[b] Department of Physics, University of Durham, Durham, DH1 3LE

Abstract

We study the properties of dijet production in deep inelastic scattering using a unified BFKL/DGLAP framework, which includes important subleading $\ln(1/x)$ contributions. We calculate the azimuthal decorrelation between the jets. We compute the cross section for dijet production as a function of Q^2 and the jet transverse momentum, as well as calculate the total dijet rate. We compare the predictions with HERA data.

arXiv:hep-ph/9904402v1 20 Apr 1999

Dijet production in high energy deep inelastic electron-proton scattering can expose properties of small x behaviour in QCD, as can be seen from Fig. 1. In the dominant $\gamma^* g \to q\bar{q} \to$ dijet subprocess, the incoming gluon can have sizeable transverse momentum accumulated from diffusion in k_T along the gluon chain [1, 2]. The value of the transverse momentum, and hence the azimuthal decorrelation between the jets, increases with decreasing x. That is the jets are no longer back-to-back since they must balance the appreciable transverse momentum k_T of the incoming virtual gluon. The azimuthal decorrelation from the back-to-back configuration $\phi = \pi$ is therefore a measure of k_T and may be expected to be an indicator of the diffusion along the BFKL chain. Clearly to obtain a reliable measure we must avoid the infrared region $k_T \simeq 0$ (that is $\phi \simeq \pi$). However, as will be seen, we are able to make an essentially parameter-free prediction of the integrated dijet production rate (at the parton level).

The description of dijet production is based on the unfolded k_T factorization formula for structure functions [3, 4], which exposes the unintegrated gluon distribution $f(x_g, k_T^2)$ more locally than the structure functions themselves. The calculation goes beyond the conventional (fixed order) QCD-improved parton model, which is known to underestimate the dijet rate [5]. We will find that the approach driven by the unintegrated gluon distribution gives an enhancement in the predicted rate and hence an improvement in comparison with the data.

The differential cross section for producing two jets of transverse momenta p_{1T} and p_{2T} in deep inelastic scattering is

$$\frac{d\sigma}{dx dQ^2 d\phi dp_{1T}^2 dp_{2T}^2} = \frac{4\pi\alpha^2}{xQ^2} \left[\left(1 - y - \frac{y^2}{2}\right) \frac{dF_T}{d\phi dp_{1T}^2 dp_{2T}^2} + (1-y) \frac{dF_L}{d\phi dp_{1T}^2 dp_{2T}^2} \right] \quad (1)$$

where, as usual, the deep inelastic variables $Q^2 = -q^2$, $x = Q^2/2p\cdot q$ and $y = p\cdot q/p\cdot p_e$ where p_e, p and q are the four momenta of the incident electron, proton and virtual photon respectively, see Fig. 1. The differential structure functions are obtained from the k_T factorization prescription by unfolding the integrations over p_{1T}^2, p_{2T}^2 and the azimuthal angle ϕ between the q and $\bar{q}$ jets.

It is convenient to use a Sudakov decomposition of the jet four momenta

$$p_1 = (1 - \beta)q' + \alpha_1 p + \boldsymbol{p}_{1T}$$

$$p_2 = \beta q' + \alpha_2 p + \boldsymbol{p}_{2T}$$

(2)

where $q' = q + xp$ and p are the basic lightlike momenta. Since the jets are on-mass-shell

$$\alpha_1 = \left(\frac{p_{1T}^2 + m_q^2}{(1-\beta)Q^2}\right) x, \qquad \alpha_2 = \left(\frac{p_{2T}^2 + m_q^2}{\beta Q^2}\right) x \quad (3)$$

where m_q is the mass of the quark. The k_T factorization formula for the differential structure functions is

$$\frac{dF_i}{d\phi dp_{1T}^2 dp_{2T}^2} = \sum_q \int_0^1 d\beta \, \mathcal{F}_i^q(\beta, p_{1T}^2, p_{2T}^2, \phi, Q^2) \frac{f(x_g, k_T^2)}{k_T^4} \quad (4)$$

1

with $i = T, L$. The function $f(x_g, k_T^2)$ is the unintegrated gluon distribution describing the gluon chain in Fig. 1. The variables x_g and k_T are the longitudinal momentum fraction and the transverse momentum, relative to the proton, carried by the gluon which couples to the $q\bar{q}$ jet pair. They are given by

$$x_g = x + \alpha_1 + \alpha_2 \qquad (\gtrsim [1 + 4p_{iT}^2/Q^2]x)$$

$$k_T^2 = p_{1T}^2 + p_{2T}^2 + 2p_{1T}p_{2T}\cos\phi,$$

(5)

see Fig. 1. The functions $\mathcal{F}_i$, which describe the virtual photon-gluon fusion subprocess $\gamma g \to q\bar{q}$, are

$$\mathcal{F}_T^q = e_q^2 \alpha_S(k_T^2)\frac{Q^2}{8\pi^2}\left\{\left[\beta^2 + (1-\beta)^2\right]\left(\frac{p_{1T}^2}{D_1^2} + \frac{p_{2T}^2}{D_2^2} + \frac{2p_{1T}p_{2T}\cos\phi}{D_1 D_2}\right) + m_q^2\left(\frac{1}{D_1} - \frac{1}{D_2}\right)^2\right\}$$ (6)

$$\mathcal{F}_L^q = e_q^2 \alpha_S(k_T^2)\frac{Q^4}{2\pi^2}\beta^2(1-\beta)^2\left(\frac{1}{D_1} - \frac{1}{D_2}\right)^2$$ (7)

where e_q is the charge of the quark and where the denominators

$$D_i = p_{iT}^2 + m_q^2 + \beta(1-\beta)Q^2.$$ (8)

The unintegrated gluon distribution $f(x_g, k_T^2)$ is obtained by using a unified BFKL/DGLAP formalism, which includes sub-leading $\ln(1/x_g)$ contributions[1], to fit to the inclusive F_2 structure function data [9]. In this way $f(x_g, k_T^2)$ is determined for $k_T^2 > k_0^2$ where $k_0^2 = 1$ GeV^2. Formally the integration limits for β in (4) are 0 and 1, but they are constrained by the condition $x_g < 1$. Moreover the lower limit on k_T in the determination of the unintegrated gluon means that we cannot predict the azimuthal decorrelation between the jets in the near back-to-back domain $\phi \simeq \pi$. Our decorrelation predictions are limited to the region

$$1 + \cos\phi > k_0^2/2p_0^2$$ (9)

where p_0 is the minimal value of the transverse momentum of an outgoing jet in the dijet system.

Predictions for the azimuthal decorrelation are shown in Fig. 2. They are compared with the measurements made using the ZEUS detector which so far have been presented in the thesis of Przybycien [5]. We use the parton level data obtained with the k_T jet-finding algorithm. The predictions use the same cuts as the data; that is $Q^2 > 8$ GeV^2, outgoing electron energy < 10 GeV, $p_T(\text{jet}) < 4$ GeV, $-2 < \eta(\text{lab}) < 2.2$ and $\eta(\text{HCM}) > 0$, where the pseudorapidities

---

[1]Next-to-leading order (NLO) $\ln(1/x)$ corrections are known to be large [6, 7], and imply the need for an all-order resummation. We are able to include a major part of the all-order resummation by imposing a consistency constraint on the BFKL kernel [8]. The constraint requires the virtuality of the exchanged gluons along the chain to be dominated by their transverse momentum squared. Although the constraint contributes at all orders, its NLO contribution gives about 70% of the exact NLO result for the BFKL Pomeron intercept.

η refer to the HERA and hadron centre-of-mass frames respectively. In each x bin the data for the ϕ distribution are normalized to unity, and the predictions are normalized to the data point centred at $\phi = 2.55$ radians ($\phi = 146°$). We see that there is satisfactory agreement between the predictions and the shape of the observed ϕ distributions. It should, however, be noted that, due to the cuts, eq. (5) implies that $x_g \gtrsim 9x$. Thus the observed x bins do not fully expose the small x_g domain. Hence the broadening of the azimuthal decorrelation, although visible in the predictions, is quantitatively marginal. The x_g distribution of the data is compared with the predictions in Fig. 3(a). We see these data sample the gluon in the region $x_g \simeq 10^{-2}$. Not surprisingly, in this x_g domain the ϕ distribution does not give a definitive test of the underlying dynamics. Indeed Monte Carlos, which do not embody BFKL effects, can also describe the ϕ distribution reasonably well [5].

We emphasize that the calculation of dijet production is essentially parameter free. Moreover it applies to the full kinematic domain since it is based on an unintegrated gluon which is obtained from a unified BFKL/DGLAP approach. The parameters which enter the determination of the unintegrated gluon are completely specified by the fit to the F_2 structure function data [9]. Thus we can make an absolute comparison with the measured cross section for dijet production. Fig. 3(b) shows the comparison as a function of Q^2. At large Q^2 there is excellent agreement. However as Q^2 decreases the prediction, with its weaker Q^2 dependence, falls below the data. The reason is that for $Q^2 \ll 4p_{iT}^2$ the denominators D_i of (8) are dominated by p_{iT}^2 and hence the calculated cross section depends only weakly on Q^2. There is a natural explanation of the discrepancy in Fig. 3(b). Dijets may also be produced in the photon hemisphere from the higher order contribution in which one of the jets is a gluon emitted from the quark box, that is $\gamma g \to gq(\bar{q})$ or $g\bar{q}(q)$ with a spectator $\bar{q}$ or q of small p_T. We expect a more rapid Q^2 fall-off from such a contribution.

In order to calculate the x_g and Q^2 distributions of Fig. 3 we integrate over the entire k_T^2 range of the gluon. The infrared contribution from $k_T^2 < k_0^2$ is estimated using the prescription of ref. [9]. That is we use the strong-ordering approximation $k_T^2 \ll p_T^2$ and express the corresponding integrals in terms of the integrated gluon distribution $g(x_g, k_0^2)$ at scale k_0^2. This non-perturbative input is determined by the fit to the F_2 data in a self-consistent way in the unified BFKL/DGLAP framework [9].

In Table 1 we make the comparison of the data and the predictions of the dijet cross section for different values of the minimal p_T of the jets. The calculation reproduces 70–80% of the observed rate. To put this comparison in context, we note that the Mepjet Monte Carlo predicts a dijet cross section for $p_T(\text{jet}) > 4$ GeV of 2.8^2 or 2.6 nb according to whether GRV [10] or MRSA [11] partons were used [5]. The latter set of partons have an integrated gluon more compatible with that used for our analysis. Thus the inclusion of small x contributions are seen to enhance the cross section, although the prediction of 3.2 nb is still below the measured value of 3.9 nb.

---

[2]This number corresponds to Mepjet 2.0 with Q as the scale. If p_T is taken to be the scale the cross section drops to 2.4 nb [5].

p_T in GeV	σ (expt) in nb	σ (theory) in nb
4	3.9	3.2
5	2.6	1.8
6	1.6	1.1
7	1.0	0.7
8	0.6	0.5

Table 1: The comparison of the measured [5] and theoretical integrated dijet production cross sections at the parton level for different p_T cuts on the jet transverse momenta in the hadronic centre-of-mass frame.

In principle dijet production appears to offer an opportunity to study the k_T diffusion property of the BFKL gluon $f(x_g, k_T^2)$. In practice the cuts, necessary on the transverse momentum of the jets, curtail the small x_g "reach" of HERA, see (5). Fortunately our unified BFKL/DGLAP approach is not restricted to small x_g, and gives a satisfactory description of the azimuthal decorrelations of the jets. Not surprisingly, the description is not unique and several standard Monte Carlos are known to also be able to accommodate the decorrelation data. The ϕ distribution, in the presently accessible kinematic domain, cannot therefore be regarded as a discriminator of the underlying small x dynamics. However our BFKL/DGLAP framework (with subleading $\ln(1/x)$ contributions) does give an enhancement of the dijet rate, although the prediction still falls short of the observed cross section. Moreover by comparing the predicted Q^2 dependence of the cross section with the data we are able to reveal the potential source of the remaining discrepancy.

Acknowledgements

References

[1] A.J. Askew, D. Graudenz, J. Kwiecinski and A.D. Martin, Phys. Lett. **B338** (1994) 92.

[2] J.R. Forshaw and R.G. Roberts, Phys. Lett. **B335** (1994) 494.

[3] S. Catani, M. Ciafaloni and F. Hautmann, Phys. Lett. **B242** (1990) 97; Nucl. Phys. **B366** (1991) 135; S. Catani and F. Hautmann, Nucl. Phys. **B427** (1994) 475; M. Ciafaloni and D. Colferai, `hep-ph/9806350`.

[4] J.C. Collins and R.K. Ellis, Nucl. Phys. **B360** (1991) 3.

[5] M. Przybycien, Ph.D. thesis "Two jets production in neutral current deep inelastic e^+p interactions at 300 GeV c.m.s. energy", Krakow, Dec. 1998.

[6] V.S. Fadin, M.I. Kotskii and R. Fiore, Phys. Lett. **B359** (1995) 181; V.S. Fadin, M.I. Kotskii and L.N. Lipatov, `hep-ph/9704267`; V.S. Fadin, R. Fiore, A. Flachi and M.I. Kotskii, Phys. Lett. **B422** (1998) 287; V.S. Fadin and L.N. Lipatov, `hep-ph/9802290`; Phys. Lett. **B429** (1998) 127; V.S. Fadin, `hep-ph/9807527`, `hep-ph/9807528`; M. Ciafaloni and G. Camici, Phys. Lett. **B386** (1996) 341; **B412** (1997) 396; **B417** (1998) 390 (E); Phys. Lett. **B430** (1998) 349; M. Ciafaloni, `hep-ph/9709390`.

[7] D.A. Ross, Phys. Lett. **B431** (1998) 161;
G.P. Salam, JHEP **9807** (1998) 019.

[8] J. Kwiecinski, A.D. Martin and P.J. Sutton, Z. Phys. **C71** (1996) 585.

[9] J. Kwiecinski, A.D. Martin and A.M. Stasto, Phys. Rev. **D56** (1997) 3991.

[10] M. Glück, E. Reya and A. Vogt, Z. Phys. **C67** (1995) 433.

[11] A.D. Martin, R.G. Roberts and W.J. Stirling, Phys. Rev. **D50** (1994) 6734.

Figure Captions

Fig. 1 Diagrammatic representation of dijet production in deep inelastic scattering via the photon-gluon subprocess. It defines the kinematics and dynamical quantities entering the k_T factorization formula (4).

Fig. 2 Theoretical predictions for the distribution with respect to the azimuthal angle ϕ between the q and $\bar{q}$ jets, compared to the data of ref. [5], for three different intervals of Bjorken x. The data are at the parton level and were obtained using the k_T jet-finding algorithm. The predictions are normalised to the data point at $\phi = 2.55$ radians.

Fig. 3 Theoretical predictions for (a) the x_g dependence, and (b) the Q^2 dependence, of the dijet production cross section compared to the parton-level data of ref. [5].
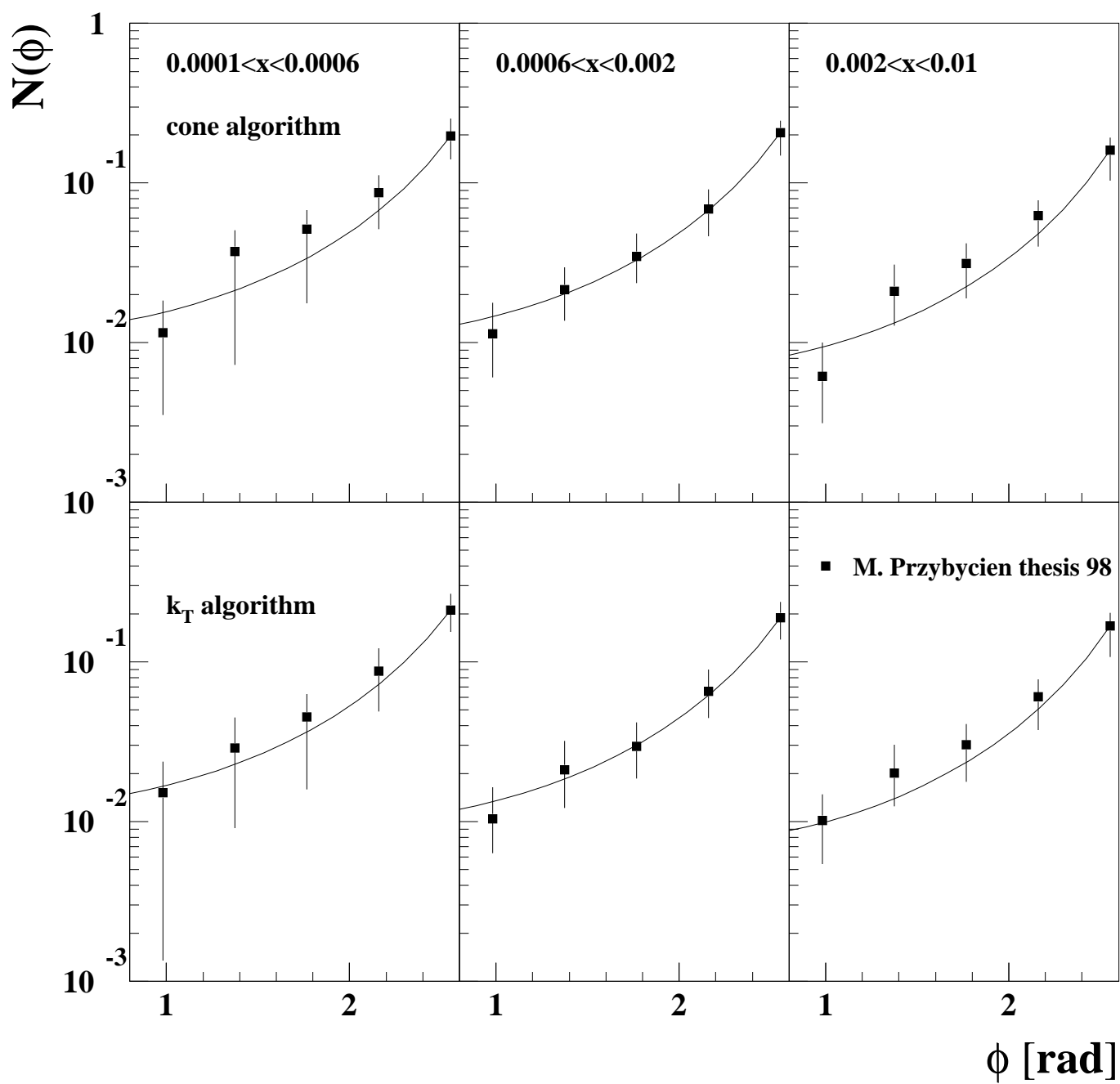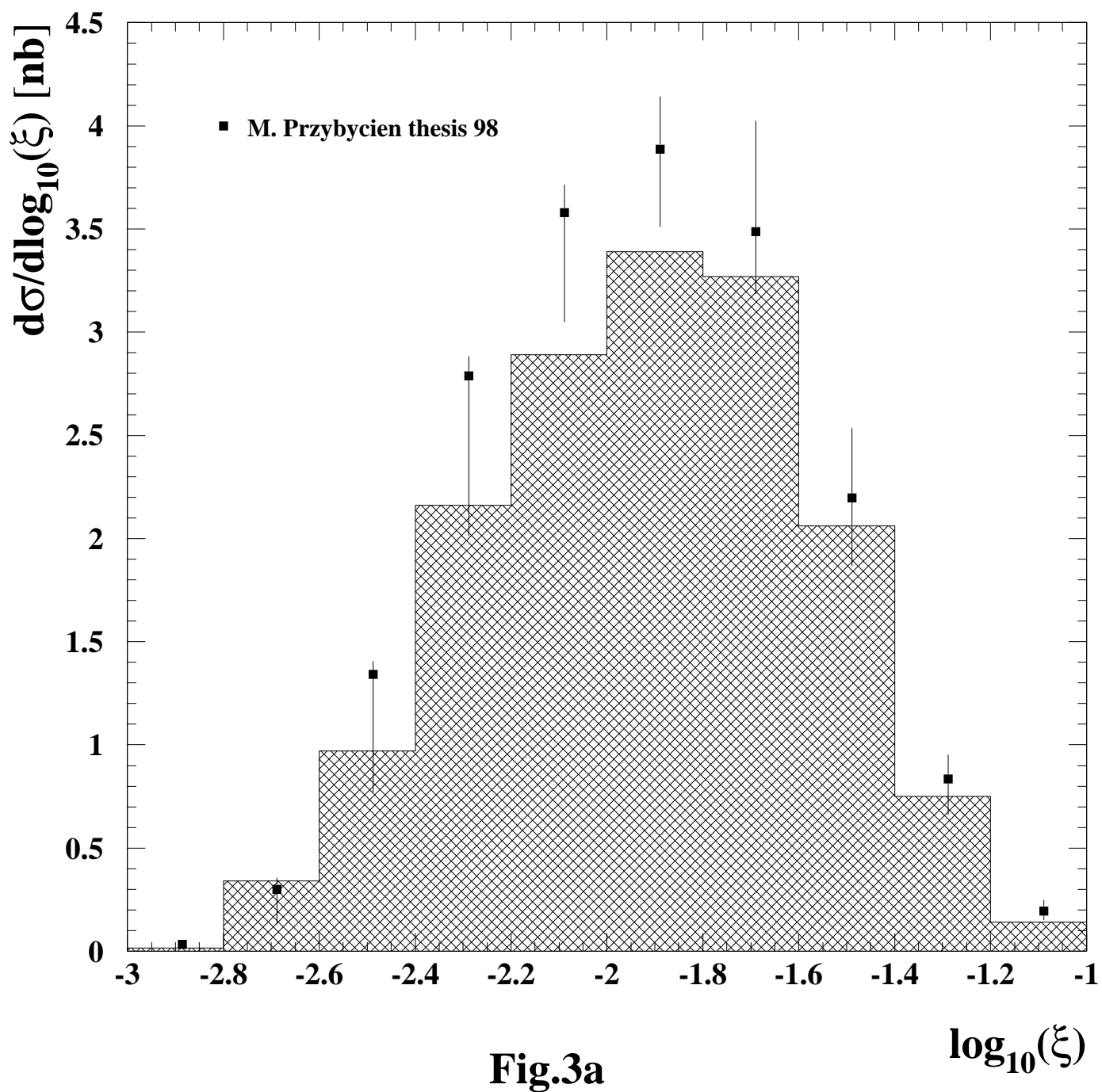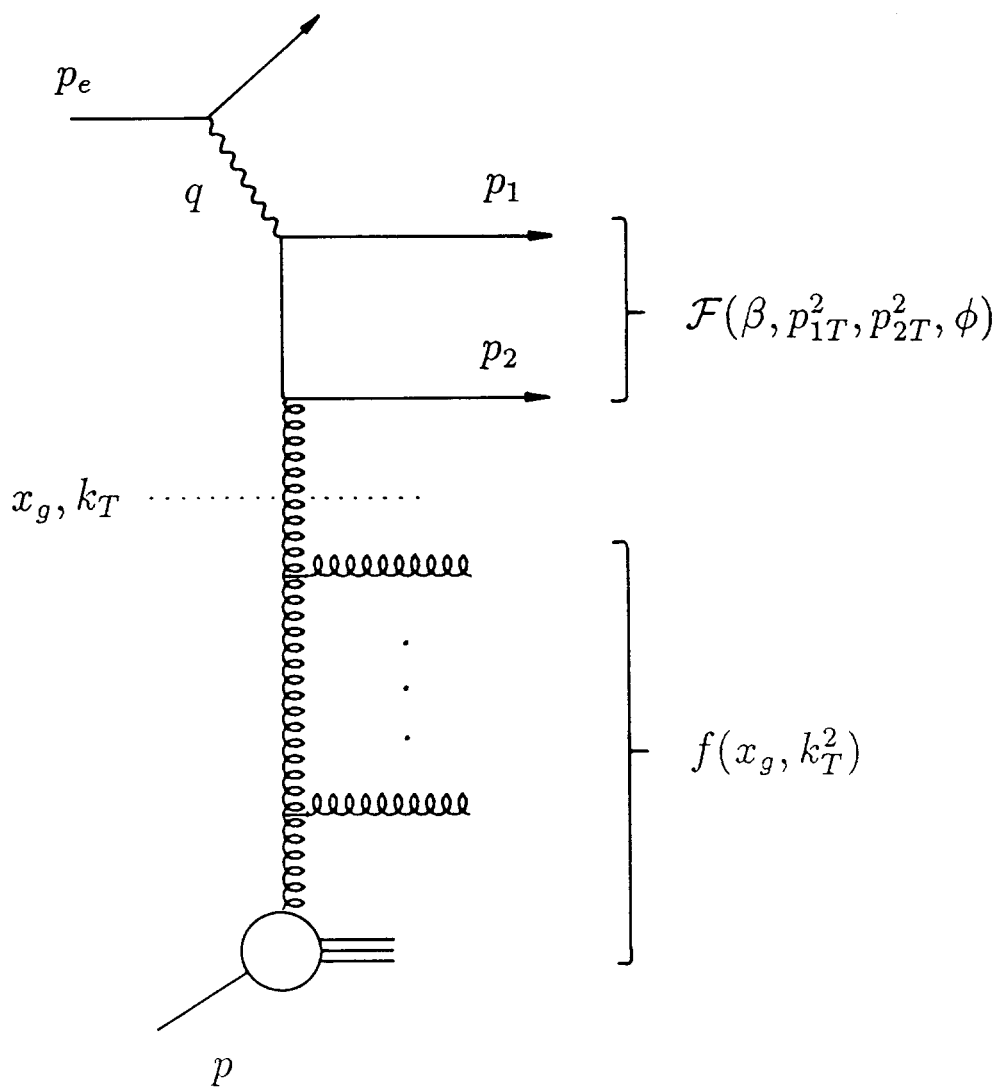
Fig.2

Fig.3a

Fig.1

Fig.3b